*ISSN 0018-151X, High Temperature, 2015, Vol. 53, No. 3, pp. 445–452. © Pleiades Publishing, Ltd., 2015.*
*Original Russian Text © A.S. Askarova, V.E. Messerle, A.B. Ustimenko, S.A. Bolegenova, V.Yu. Maximov, Z.Kh. Gabitova, 2015, published in Teplofizika Vysokikh Temperatur, 2015, Vol. 53, No. 3, pp. 467–474.*

## HIGH TEMPERATURE APPARATUSES AND STRUCTURES

# Numerical Simulation of Pulverized Coal Combustion in a Power Boiler Furnace

**A. S. Askarova[a], V. E. Messerle[b], A. B. Ustimenko[a], S. A. Bolegenova[a], V. Yu. Maximov[a], and Z. Kh. Gabitova[a]**

[a] *Research Institute of Experimental and Theoretical Physics, Al-Farabi Kazakh National University, Almaty, Kazakhstan*
[b] *Kutateladze Institute of Thermal Physics, Siberian Branch, Russian Academy of Sciences, Novosibirsk, Russia*
*e-mail: ust@physics.kz*

Received January 6, 2014

**Abstract**—Investigation of the combustion of the coal-dust flame in a BKZ-75 boiler furnace of the Shakhtinskaya thermal power station (TPS) is carried out using three-dimensional simulation. The distributions of the full velocity vector and the temperature and components concentration profiles, including hazardous pollutants, in the furnace volume and at its outlet are determined. It is shown that swirling flows of the air–fuel mixture that enters the furnace through contradirectional burners form a volume vortex flow in the central section. The maximum concentrations of combustion products in the area of arrangement of burner devices are observed in the cross section of the body of the flame. The concentrations of hazardous pollutants at the furnace outlet are less than the admissible concentrations accepted for the TPS.

**DOI:** 10.1134/S0018151X15020030

## INTRODUCTION

In the immediate term, one would expect a substantial increase in the fraction of solid fuel in the power output of thermal power stations (TPS) of the Republic of Kazakhstan. Boiler installations for high-output power units on coals of existing and new coalfields will be developed to replace the outdated equipment. From the experience of the adoption of new power pulverized-coal units, the investigation of furnace processes in large-scale boiler plants for their improvement is extremely difficult. To enhance the reliability and to improve the design quality, of great engineering importance is the development of methods for complex designs of furnace devices with consideration of the aerodynamics, ignition, burning of the coal-dust flame, heat exchange, and the chemical kinetics of combustion product generation.

Modernization of power boilers with small and average powers for purposes of more rational fuel combustion, enhancement of the efficiency of heat transfer from a surface, and the possibility for low-calorie solid fuel combustion is economically more advantageous than their full replacement [1]. In recent years, the design and modernization of boilers, industrial furnaces, and combustion chambers have been carried out with broad application of computer three-dimensional simulation based on mathematical heat and mass transfer with consideration of the chemical reactions within the furnace space using the fundamental laws of physics and chemical thermodynamics enhanced by the corresponding models of turbulence and chemical kinetics. The application of three-dimensional simulation makes it possible to investigate numerically nonlinear physical processes of hydrodynamics and heat and mass transfer with consideration of physicochemical phenomena: combustion, radiation heat transfer, and heightened turbulence [2, 3]. In view of this situation, the aim of this study is numerical simulation of pulverized coal combustion in a BKZ-75 boiler furnace of the Shakhtinskaya TPS for purposes of enhancing its efficiency due to an increase in the completeness of fuel burn-out ($CO_2$ concentration) and a decrease in the chemical underburning of the fuel (CO concentration) and nitrogen oxide ($NO_x$) emission into the environment. The results of numerical simulation make it possible to optimize the furnace configuration and the arrangement and construction of pulverized-coal burners and to develop engineering solutions based on it for effective burning of power-generating coals.

For numerical simulation of the temperature, aerodynamic, and concentration characteristics of coal combustion, we choose the BKZ-75 power boiler furnace of the Shakhtinskaya TPS (Kazakhstan) with the following technical characteristics [4]. The Shakhtinskaya TPS is equipped with four BKZ-75 boilers with a steam capacity of 75 t/h. The BKZ-75 boiler of the Shakhtinskaya TPS (Fig. 1a) is equipped with four swirl pulverized-coal burners (Fig. 1b) mounted by two from the front and the back in one tier. The boiler furnace burns the dust of the Karaganda common (KR-200) coal with an ash content of 35.1%, devolatilization degree of 22%, humidity of 10.6%, and combustion heat of 18 550 kJ/kg.

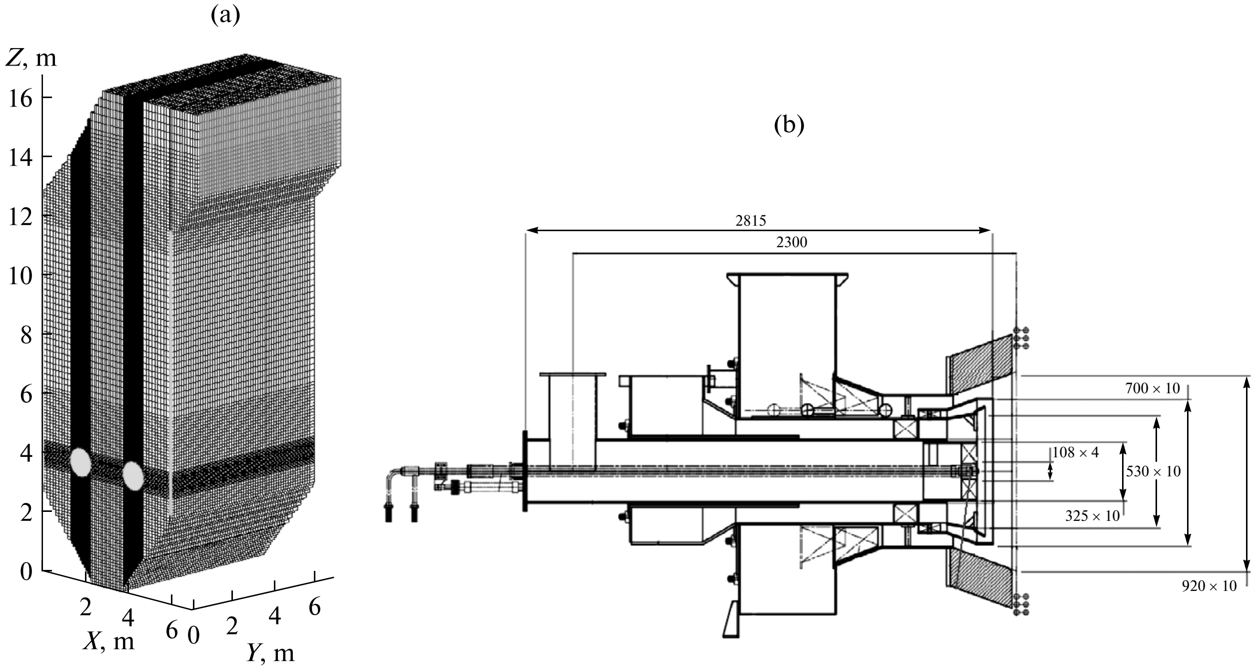

**Fig. 1.** General view of (a) the BKZ-75 boiler furnace of the Shakhtinskaya TPS and (b) the pulverized coal burner.

## MODEL OF PHYSICOCHEMICAL PROCESSES

In the present study chemical, mathematical, and physical models were used to investigate heat and mass transfer in high-temperature media with physicochemical processes occurring in them. These models include a set of three-dimensional Navier–Stokes equations and heat and mass transfer equations subject to source terms, which are determined by chemical kinetics of the process, nonlinear effects of thermal radiation, interfacial interaction, and the many stages of chemical reactions. Let us write the general equations used for solving the formulated problem:

—mass conservation law (continuity equation)

$$\frac{\partial \rho}{\partial t} + \frac{\partial}{\partial x_i}(\rho u_i) = 0;$$

—momentum conservation law (Navier–Stokes equation)

$$\frac{\partial}{\partial t}(\rho u_i) = -\frac{\partial}{\partial x_j}(\rho u_i u_j) + \frac{\partial \tau_{ij}}{\partial x_j} - \frac{\partial P}{\partial x_i} + \rho f_i,$$

where ρ is the density; $u_{i,j}$ is the velocity in directions $i,j$; $x_{i,j}$ are the Cartesian coordinates, $\tau_{i,j}$ is the viscous stress tensor, $P$ is the pressure, and $f_i$ are external forces;

—the law of energy conservation (first law of thermodynamics)

$$\frac{\partial}{\partial t}(\rho h) = \frac{\partial}{\partial x_i}(\rho u_i h) - \frac{\partial q_i^{\text{res}}}{\partial x_j} + \frac{\partial P}{\partial t} + u_i \frac{\partial P}{\partial x_i} + \tau_{ij} \frac{\partial u_j}{\partial x_i} + S_h,$$

where $h$ is the specific enthalpy, $q_i^{\text{res}}$ is related to energy transfer due to heat conduction of substance flow and diffusion, and $S_h$ is the energy source due to chemical reactions and radiation heat transfer;

—and the law of mixture components conservation

$$\frac{\partial}{\partial t}(\rho C_\beta) = -\frac{\partial}{\partial x_i}(\rho C_\beta u_i) + \frac{\partial j_i}{\partial x_i} + S_\beta,$$

where $C_\beta$ is the mass concentration of component β, $j_i$ is the mass-averaged flow in the $i$th direction, and $S_\beta$ is the source term of component β.

The procedure based on the Euler approach was used to describe the flow and heat and mass transfer of the gas phase. This procedure uses spatial equations of the balance of mass, momentum, gas component concentrations, and energies for the gas mixture. To describe the motion and heat and mass transfer of single particles of fuels along their trajectories, the Lagrange approach [5] is used. The turbulent flow structure is described by the $k$–ε turbulence model, where $k$ is the kinetic energy of turbulence, and ε is the turbulent energy of dissipation. Radiation heat transfer is represented by a six-flow transport model [6, 7].

The mentioned set of equations is solved numerically with the modern methods of 3D simulation.

For the simulation of the formation of combustion products in the coal-dust flame, the kinetic model of chemical transformations was applied, which is true for a wide range of temperatures and reagent concentrations. However, detailed simulation of all the reactions occurring (including all the intermediate reactions) is possible only in simple cases, such as, for example, during carbon monoxide burning because of the great computational consumption or the absence of information on all intermediate reactions.

Use of the model of the integral reaction is based on the fact that most chemical reactions occur in several steps, and the slowest step of the reaction determines the rate of the entire reaction. A great number of multistage reactions can be modeled using laws of single-step reactions, and the kinetic data in such case are determined by the slowest step of the reaction. The model of coal dust combustion used in the present study takes into account the integral reactions of fuel component oxidation to stable final reaction products [8]. At the same time, the intermediate reactions, formation, and change of unstable intermediate products are not considered.

Here, the combustion model is considered in the form of the following steps:

—pyrolysis with the output of volatile substances and the formation of the carbon residue,

—combustion of volatile products and carbon monoxide,

—and combustion of carbon residue.

### *Pyrolysis Simulation*

The combustion model must exclusively describe the local heat release as a result of combustion and the effect of combustion products on heat transfer. Therefore, we rejected the application of cumbersome systems with a great number of components when choosing models of pyrolysis and combustion.

This study uses the single-step pyrolysis model described in [9, 10] because in this case the stoichiometric coefficients of the pyrolysis reaction can be derived from the data of proximate analysis that is significant and preferential. In addition, this model operates sufficiently accuracy in many cases and is a good compromise for decreasing computational costs.

### *Simulation of Volatile Substance Combustion*

Pyrolysis products mixing with air form a chemically responsive mixture. The combustion reaction rates of these gaseous products are so high that the approximation of diffusion combustion is admissible. Volatile substances are considered during the description of pyrolysis as fictitious hydrocarbons. Because only the rate and heat release during oxidation is of primary interest, volatile substance combustion at high temperatures and the substantial amount of oxygen can be represented in the form of the two-stage reaction under the assumption that first the oxidation of volatile substances to CO and $H_2O$ occurs [10],

$$C_xH_y + \left(\frac{x}{2} + \frac{y}{4}\right)O_2 \to xCO + \frac{y}{2}H_2O, \quad (1)$$

and at the second step the oxidation to $CO_2$ takes place [11, 12]:

$$xCO + \frac{x}{2}O_2 \to xCO_2. \quad (2)$$

In the study subject to reactions (1) and (2), the burning rate of pyrolysis products is determined using the concept of turbulent dissipation (Eddy-Dissipation Model, EDM) proposed by Magnussen and considered in detail in [8] in the approximation of instantaneous mixing, in which there is no necessity additionally to solve the transport equation. The given model basis is the assumption that large-scale vortices characterized by turbulent energy $k$ accelerate macromixing and turbulence energy dissipation $\varepsilon$ accelerates micromixing. Consequently, the burning rate of pyrolysis products can be related to characteristics $k$–$\varepsilon$.

### *Simulation of Carbon Residue Combustion*

The heterogeneous reaction of solid carbon combustion at the coke particle surface is determined by oxygen diffusion from the environment into the boundary layer and into the porous medium of the particle and the reaction between carbon and oxygen at the particle surface as well. The slowest process among them determines the coke burning rate. Carbon monoxide and dioxide form depending on the diameter and temperature of particles [13]:

$$C + O_2 \to 2CO,$$

$$2CO + O_2 \to 2CO_2.$$

It is suggested that the fuel particle diameter changes from $d_1$ to $d_2$ during carbon residue combustion. The particle size is invariable during the output of volatile components, and only the fuel density changes from dry coal density $\rho_1$ to coke density $\rho_2$:

$$d_2 = d_1\left[\frac{A_p}{(1-W_p)(1-f_n)}\right]^{0.333},$$

$$\rho_2 = \rho_1(1-f_n),$$

where $A_p$ and $W_p$ are the ash content and humidity after milling and $f_n$ is the mass fraction of volatile substances in dry coal.

The change of carbon concentration $\xi_C$ in coke is determined by the equation

$$\frac{d\xi_C}{dt} = -K_C A_{sp}\xi_C,$$

where $K_C$ is the oxidation rate constant of coke residue carbon and $A_{sp}$ is the specific particle surface related to its mass.

For the $n$th order reaction, we have the relation

$$K_C = K_{kin}\left(p_{O_2} - \frac{K_C}{K_d}\right)^n.$$

Here, $K_{kin}$ is the rate constant of the kinetic component of the coke carbon combustion reaction, $K_d$ is the oxidized diffusion rate constant, and $p_{O_2}$ is the relative partial pressure of oxygen. Reaction order $n$ takes the following magnitudes: 1 for black coal and 0.5 for

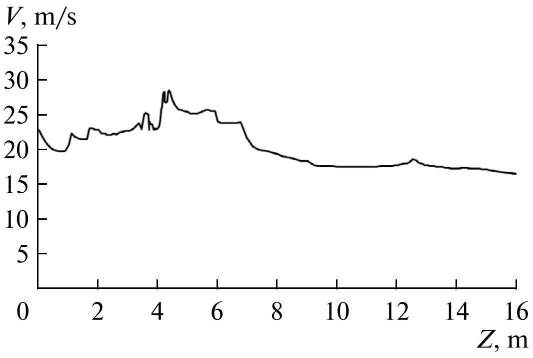

**Fig. 2.** Distribution of the full velocity vector in the central section over the furnace height.

brown coal. Then, for example, the equation for black coal is

$$K_{\mathrm{C}} = \frac{p_{\mathrm{O}_2}}{\dfrac{1}{K_d} + \dfrac{1}{K_{\mathrm{kin}}}}.$$

The contribution of oxygen diffusion is determined in terms of the oxidized diffusion rate constant according to [13]:

$$K_d = \frac{\mathrm{Sh} M_{\mathrm{C}} f_m D_{\mathrm{O}_2}}{R d_p T_{GS}},$$

where $M_{\mathrm{C}}$ is the molar mass of carbon; Sh is the Schwarzschild number (Sh = 2 is taken for spherical particles); $T_{GS} = \frac{T_G + T_P}{2}$ is the average temperature of the mixture; $T_G$ and $T_P$ are the temperatures of gas and solid particles, respectively; and $D_{\mathrm{O}_2} = D_{0,\mathrm{O}_2}\left(\frac{T_{GS}}{T_0}\right)^{1.75}$ is the coefficient of oxygen diffusion to the particle surface [13], where $D_{0,\mathrm{O}_2} = 3.49 \times 10^{-4}$ m$^2$/s is the self-diffusion coefficient at $T_0 = 1600$ K [14].

The contribution of chemical reactions is determined through the chemical reaction rate constant, which is expressed by the relation [15]

$$K_{\mathrm{C}} = k_{0,\mathrm{C}} e^{-\frac{E_{a,C}}{RT_p}}.$$

The kinetic parameters used in computations are taken from [15].

Thus, the *n*th-order chemical reaction of formed-coke combustion can generally be written as

$$\frac{d\xi_{\mathrm{C}}}{dt} = -\xi_{\mathrm{C}} A_{\mathrm{sp}} p_{\mathrm{O}_2}^n K_{\mathrm{kin}} \left(1 - \frac{k_{\mathrm{C}}}{K_d p_{\mathrm{O}_2}}\right)^n.$$

Nitrogen oxides (NO and $NO_2$) cause photochemical air pollution, oxidation of atmospheric humidity, and ozone depletion and are considered as the most toxic emissions [16, 17]. Reduction of the nitrogen oxide concentration at the outlet of the furnace chamber is a very significant problem in the organization and optimization of coal combustion on the TPS.

### *Formation of Nitrogen Oxides*

The formation of nitrogen oxides $NO_x$ was computed based on the model proposed in [18]. The greatest contribution to nitrogen oxide formation during coal combustion gives fuel nitrogen (fuel nitrogen oxides). Nitrogen oxides may also form from molecular nitrogen of the air (thermal nitrogen oxides). The proposed kinetic model takes into account the reactions of the release of volatile substances of coal, homogeneous combustion of hydrocarbon compounds, heterogeneous combustion of coke, and the formation of thermal and fuel nitrogen oxides.

The formation of nitrogen oxides can be represented in the following way: fuel-containing nitrogen is emitted during the thermal decomposition of the coal particle; and, at the same time, approximately 80% of bound nitrogen is gasified in the form of cyanides:

$$\mathrm{N} \rightarrow \mathrm{HCN}.$$

The cyanides formed are transformed into amines, which either react with oxygen and form NO or reduce $N_2$ from NO:

$$\mathrm{HCN} + \mathrm{H_2O} + 0.5\mathrm{O_2} \rightarrow \mathrm{NH_3} + \mathrm{CO_2},$$

$$\mathrm{NH_3} + \mathrm{O_2} \rightarrow \mathrm{NO} + \mathrm{H_2O} + 0.5\mathrm{H_2},$$

$$\mathrm{NH_3} + \mathrm{NO} \rightarrow \mathrm{N_2} + \mathrm{H_2O} + 0.5\mathrm{H_2}.$$

The residual 20% of nitrogen is oxidized immediately to NO with the rate proportional to the coke burning rate:

$$\mathrm{N} + 0.5\mathrm{O_2} \rightarrow \mathrm{NO}.$$

In addition, there are the following reactions: formation of HCN as a result of hydrocarbon interaction with NO

$$\mathrm{NO} + \mathrm{C}_x\mathrm{H}_y \rightarrow \mathrm{HCN} + \mathrm{H_2O}$$

and the heterogeneous reaction between NO and the coke particle

$$\mathrm{C} + 2\mathrm{NO} \rightarrow \mathrm{CO_2} + \mathrm{N_2}.$$

For closure of the model of nitrogen oxide, it is sufficient to determine the rates of chemical reactions conditioned changing the concentrations of $NH_3$, HCN, NO, $O_2$, coke, and volatile substances, which were taken from [19].

## RESULTS AND DISCUSSION

Numerical experiments and the creation of a database for simulation were carried out in several steps using program complexes and with application of the control volume approach (CVA). For this approach, the overall computed region is divided into control cells (volumes), in the nodes of which the above-described set of nonlinear equations is solved. The

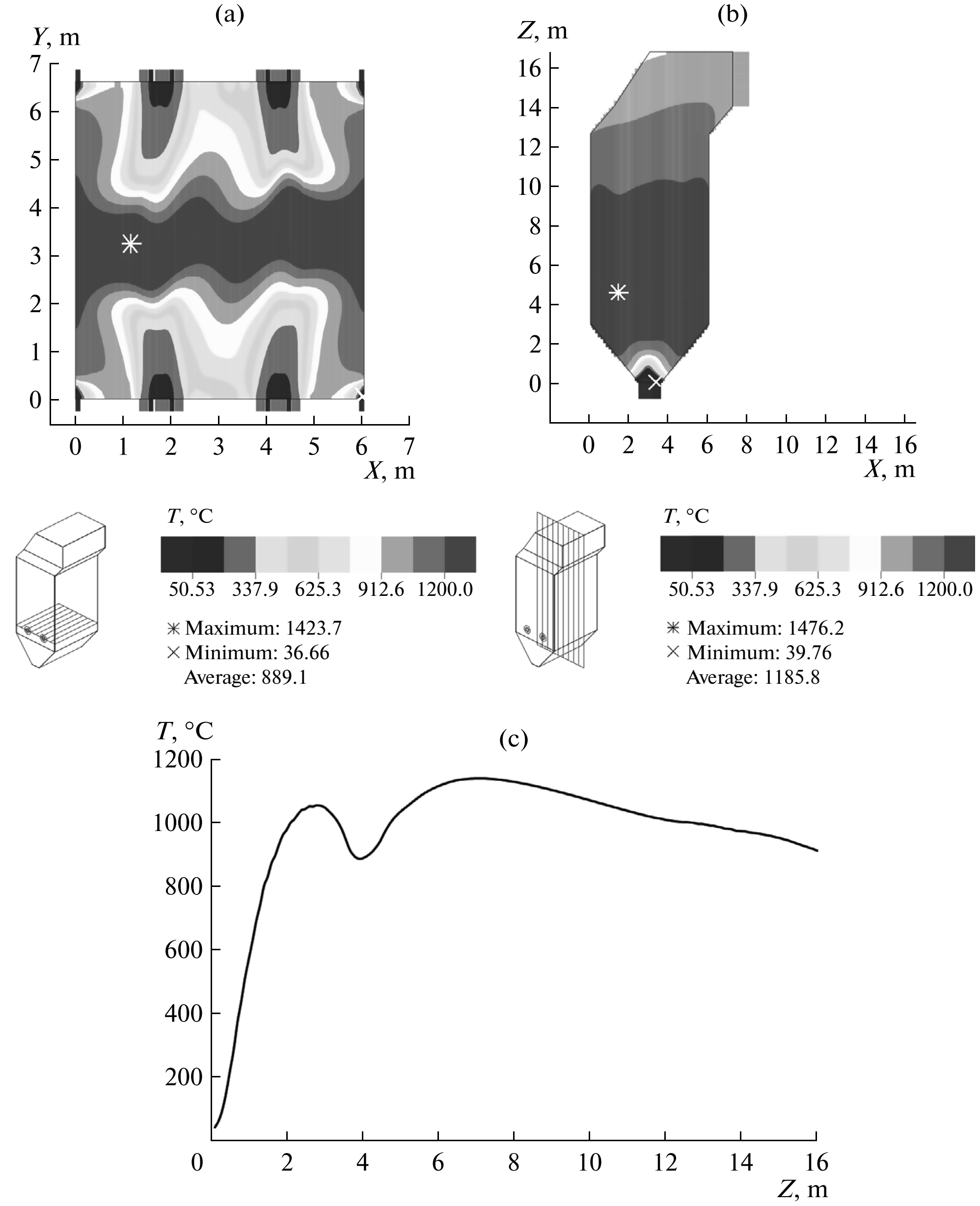

**Fig. 3.** Temperature profiles (a) at the level of the burner arrangement and (b) in the longitudinal section of the furnace, and (c) the distribution of average magnitudes of temperature over the furnace height.

BKZ-75 boiler furnace was divided into 1500000 elemental cells (Fig. 1a).

As a result of computations, we found the change in the full velocity vectors over the furnace height (Fig. 1a). One can observe regions of the supply of the fuel mixture through furnaces, in which velocity maximums are observed. The velocities decrease with distance from the level of the burner arrangement, and the velocity field is smoothed out uniformly distributed over the section of the combustion chamber. In the area of pulverized coal furnaces, we can observe intensive vortex flows evolving into direct-flow ones with movement of combustion products to the outlet of the furnace.

The temperature conditions (Fig. 3) characteristic for pulverized coal combustion in the furnace chamber form in turbulent jets and are determined by the intensity of heat and mass transfer in them and by the character of propagation of jets in the furnace. Therefore, the physical conditions of combustion in turbulent jets are determined by the laws of the distribution of temperatures and velocities [17, 20]. The maximum of convective transfer in the furnace is observed in the region of the supply of the pulverized coal mixture. Consequently, the most intensive combustion occurs

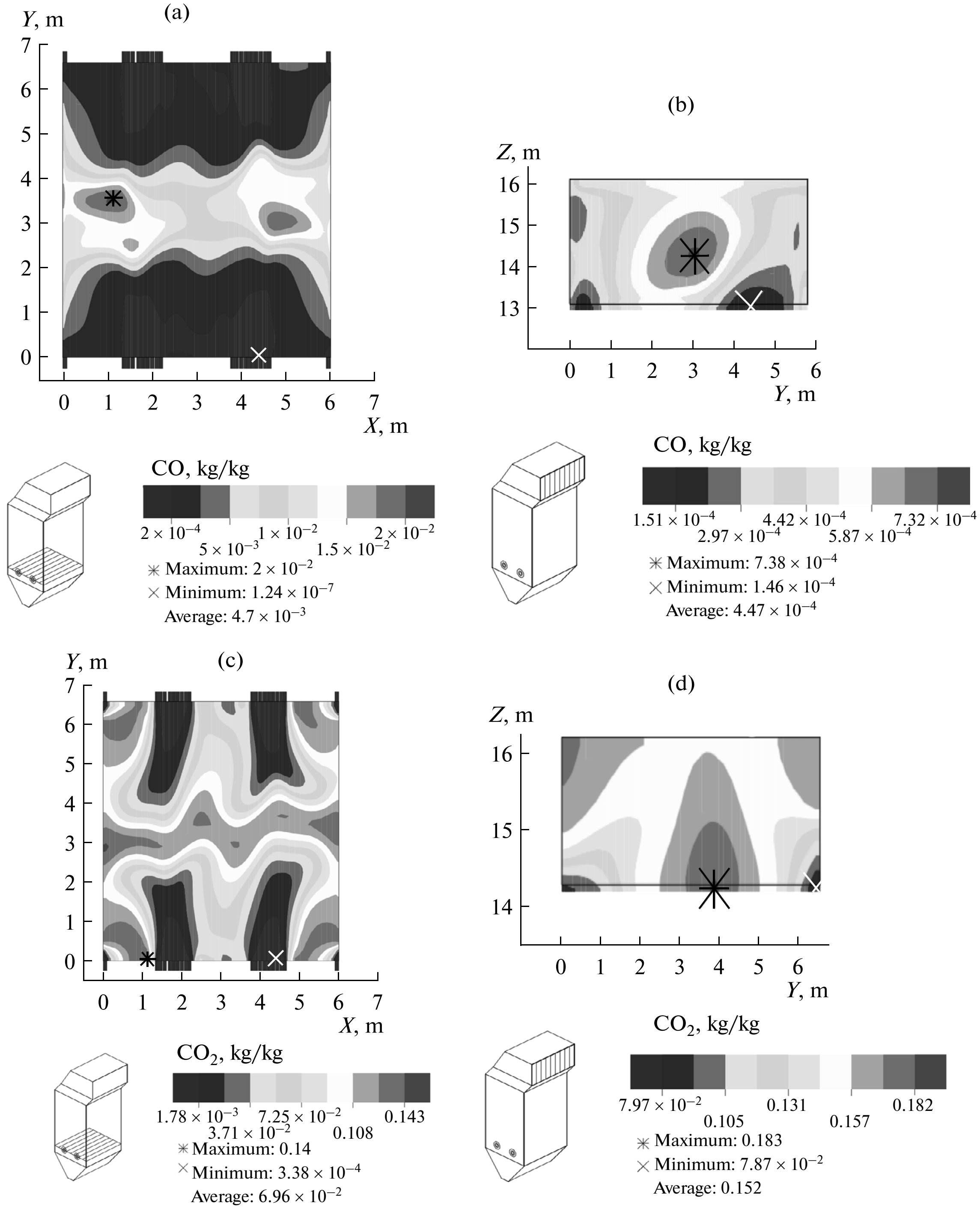

**Fig. 4.** Distribution of CO and CO$_2$ concentrations in the section (a), (b) at the level of the burner arrangement and (c), (d) at the furnace outlet.

in the central section of the furnace, which is testified to by the maximums in the temperature distribution in various sections of the combustion chamber (Fig. 3c).

Combustion reactions in the mentioned areas occur the most intensively, to which the significant changes in the temperature of this area are related. Peaks in the distribution of the temperature and its gradient are revealed near the reaction zone in the flame. The temperature decreases smoothly to the outlet of the furnace chamber (Figs. 3b, 3c).

The chemical and mechanical combustion completeness can be estimated by the concentration fields of products of chemical reactions occurring in the combustion chamber between fuel (coal) and oxidizer

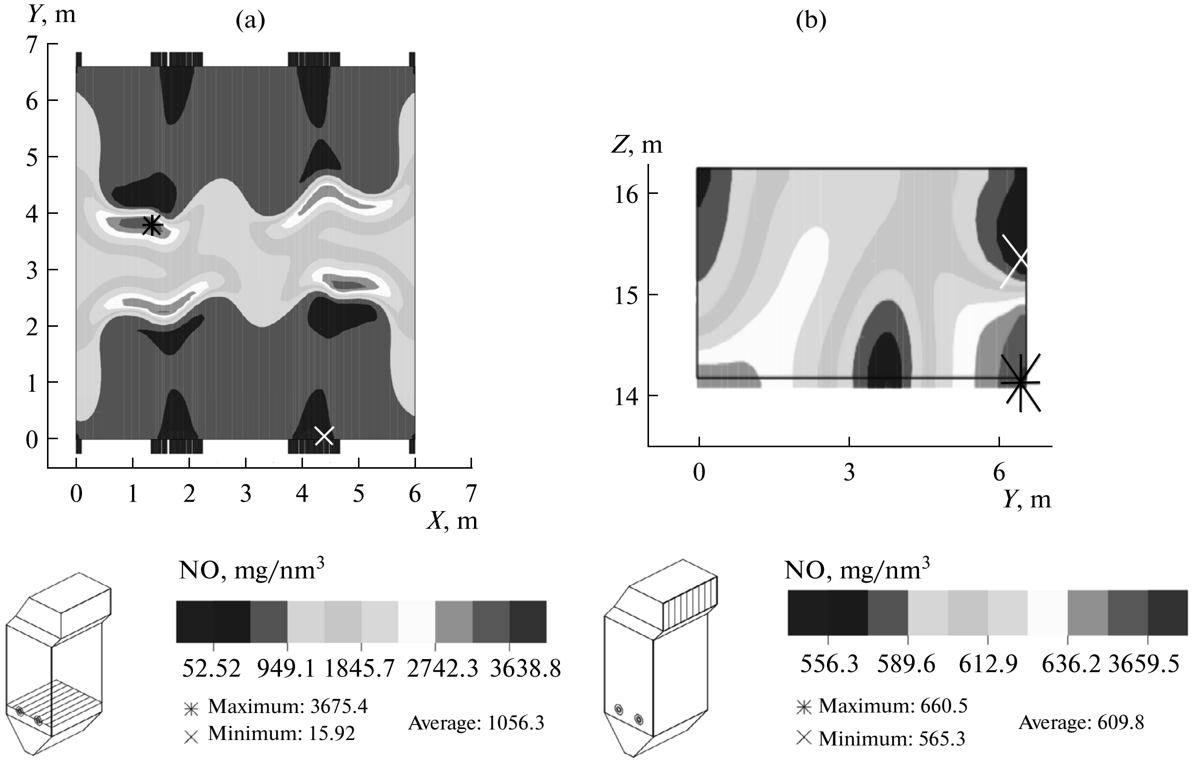

**Fig. 5.** Distribution of the NO concentration in the section (a) at the level of the burner arrangement and (b) at the furnace outlet.

(air oxygen), which can be realized by the scheme of the above-described chemical model. Carbon (CO and $CO_2$) (Fig. 4) and nitrogen (NO) (Fig. 5) oxides are the main pollutants of environment. Figure 4a shows the distribution of the carbon monoxide concentration in the furnace section at the level of the furnace arrangement. Its maximum concentration is observed in the furnace hole ($2 \times 10^{-2}$ kg/kg). Figure 4b shows the distribution of the CO concentration at the outlet of the furnace where the oxygen deficiency and the temperature is substantially lower than in the body of the flame (Fig. 3). It is evident that the chemical processes related to the intensive formation of CO are dampened. The average CO concentration at the outlet of the furnace is $4.47 \times 10^{-4}$ kg/kg, which corresponds to the maximum permissible concentrations accepted for the TPS and testifies to the chemical completeness of fuel combustion.

The distribution of the $CO_2$ concentration (Figs. 4c, 4d) differs from that considered for CO, which suggests differences in the formation of $CO_2$ and CO. It is evident that the main formation of carbon dioxide occurs with distance from the furnace center, i.e., from the area of collision of fuel and oxidizer jets of opposite burners. This shows that carbon monoxide formation depends not only on the transfer phenomenon, but on process kinetics as well. The fact of that carbon may react with oxygen in various ways is extremely significant for designing furnace chambers. Combustion technology must provide for complete mixing of the fuel with oxygen and its complete combustion with the formation of $CO_2$ and not CO. If not, heat release abrupt decreases because only 28% of energy released during the $CO_2$ formation is released during CO formation.

Figure 5 demonstrates NO concentration distributions in the furnace. The greatest NO concentrations are related to the zone of the furnace arrangement, where the body of flame and the maximum oxygen concentration is observed. For example, the maximum NO concentration in the furnace zone is 3675.4 mg/nm$^3$. The minimum NO concentration at the outlet is 565.3 mg/nm$^3$; and the section-averaged magnitude is 609.8 mg/nm$^3$, which is fully admissible for NO emission standards accepted for the TPS.

## CONCLUSIONS

(i) Swirling jets supplying fuel through opposite burners in the furnace create a volume vortex flow in the central part. The flow in furnace corners is distributed into two parts because of the direct impact on furnace walls. The main flow part goes up, and the other one goes downstream under a small angle, untwisting into two vortices. Because of the intensive vortex motion of pulverized coal flows within the furnace, the fuel particle residence time in the furnace increases substantially, which makes it possible to achieve more complete burning even during combustion of coal dust with a coarser grade.

(ii) The most intensive combustion is observed in the central part of the furnace, where the flow temperature attains the order of 1200°C. Because coal particles radiate more intensive in this area and have a higher concentration and total surface area, the temperature attains a maximum near the section of the burner arrangement. Combustion occurs most intensively precisely in this area.

(iii) Maximum concentrations of combustion products in the furnace are observed in the area of the burner arrangement in the section of the body of the flame. Emission concentrations at the outlet of the furnace do not exceed the maximum permissible concentrations accepted for Kazakhstan HPPs operating on pulverized coal.

## REFERENCES

1. Gazeev, M.Kh. and Orlov, R.V., *Elektron. Zh. Ekol. Sist.*, 2004, no. 7. http://www.esco-ecosys.narod.ru/2004_7/art11.htm.
2. Pauker, W., *Creating Data Sets for FLOREAN Using the Tool PREPROZ*, Braunschweig, Germany: IWBT, 1997.
3. Müller, H., *Numerische Berechnung dreidimensionaler turbulenter Strömungen in Dampferzeugern mit Wärmeübergang und chemischen Reaktionen am Beispiel des SNCR–Verfahrens und der Kohleverbrennung*, VDI-Fortschrittsberichte Reihe 6: Energieerzeugung, Nr. 268, 1992.
4. Askarova, A.S., Bolegenova, S., Maximov, V., Bekmukhamet, A., and Ospanova, Sh., *J. Proc. Eng.*, 2012, vol. 42, p. 1250.
5. Launder, B.E. and Spalding, D.B., *Comput. Methods Appl. Mech. Eng.*, 1974, vol. 3, no. 2, p. 269.
6. Lockwood, F. and Shah, N., in *ASME-Paper of the ASME–AIChE Heat Transfer Conference, Salt Lake City, Utah, United States, 1976*, 76–HT–55, p. 7.
7. De Marco, A.G. and Lockwood, F.C., *Riv. Combust.*, 1975, vol. 24, nos. 5–6, p. 184.
8. Müller, H., *Numerische Berechnung dreidimensionaler turbulenter Strömungen in Dampferzeugern mit Wärmeübergang und chemischen Reaktionen am Beispiel des SNCR–Verfahrens und der Kohleverbrennung*, Braunschweig, Germany: Fortschritt, 1992, Reiche 6, no. 268.
9. Harmor, R.J., *Combust. Flame*, 1973, no. 21, p. 153.
10. Edelman, R.B. and Fortune, O.F., in *Proceedings of the AIAA Seventh Aerospace Sciences Meeting, New York, January 20–22, 1969.*
11. Schnell, U., *Berechnung der Stickoxidemissionen von Kohlenstaubfeuerungen*, Braunschweig, Germany: Forschritt, 1991.
12. Magnussen, B.F., in *Works of the 16th International Symposium on Combustion, Pittsburgh, Pennsylvania, United States, 1976*, p. 719.
13. Field, M.A., Gill, D.W., Morgan, B.B., and Hawksley, P.G.W., *Combustion of Pulverized Coal*, Leatherhead, Surrey, United Kingdom: British Coal Utilisation Research Association (BCURA), 1967, p. 186.
14. Müller, H., *Numerische simulation von Feuerungen. CFD-Vorlesung, TU*, Braunschweig, Germany: IWBT, 1997.
15. Görner, K., *Technische verbrennungssysteme, Grundlagen, Modellbildung, Simulation*, Berlin: Springer-Verlag, 1991.
16. Askarova, A.S., Karpenko, V.E., Messerle, V.E., and Ustimenko, A.B., *High Energy Chem.*, 2006, vol. 40, no. 2, p. 111.
17. Askarova, A.S., Karpenko, E.I., Lavrishcheva, Y.I., Messerle, V.E., and Ustimenko, A.B., *IEEE Trans. Plasma Sci.*, 2007, vol. 35, no. 6, p. 1607.
18. Mitchell, J.W. and Tarbell, J.M., *AIChE J.*, 1982, vol. 28, p. 302.
19. Starchenko, A.V., *Combust., Explos., Shock Waves*, 1998, vol. 34, no. 6, p. 603.
20. Kudryavtsev, A.V. and Gorbatko, A.A., *High Temp.*, 2012, vol. 50, no. 5, p. 684.

*Translated by S. Ordzhonikidze*